

## Self-Organized Quasiparticles: Breathing Filaments in a Gas Discharge System

I. Müller, E. Ammelt, and H.-G. Purwins

*Institute of Applied Physics, University of Münster, Corrensstrasse 2/4, D-48149 Münster, Germany*

(Received 6 February 1998)

A quasi-two-dimensional, lateral ac-powered gas discharge system is investigated experimentally from the point of view of pattern formation. In a certain parameter range, well localized self-organized quasiparticles in the shape of current density filaments are observed. By varying the supply voltage, such objects can be destabilized and stationary filaments with a circular symmetry undergo a transition towards breathing filaments of dumbbell shape. [S0031-9007(99)08935-8]

PACS numbers: 47.54.+r, 52.80.Pi, 82.20.Mj

Localized particlelike structures in continuous non-linear systems, also referred to as spots, dissipative solitons, or autosolitons have been observed experimentally as well as theoretically under various circumstances [1–6]. Fundamental theoretical studies of self-organized quasiparticles in reaction-diffusion systems of the activator-inhibitor type have been undertaken by different authors [4,7,8]. Theoretical investigations of the breathing motions of spots and their static deformations have been carried out for activator-inhibitor systems with a piecemeal linear activator nullcline [3,9]. Well localized breathing objects have been found on an experimental basis in two-dimensional chemical systems [10]. However, these oscillations have been interpreted as an interaction of a front with the system's boundary and not as oscillations of the radius of a self-organized quasiparticle independent of the boundary. Pulsations of circular as well as of dumbbell-shaped flames have been observed in porous plug burners [11]. In lateral gas discharge systems, i.e., in systems where the lateral extension of the electrodes is large with respect to the thickness of the gas gap, self-organized quasiparticles have been known for many decades [12,13]. Only recently, however, have such systems been investigated systematically from the point of view of pattern formation [14–16].

In this paper, we present results that were obtained experimentally in a quasi-two-dimensional, lateral dielectric barrier gas discharge system. This strongly non-linear system shows a great variety of patterns. On the one hand, there are interacting solitonlike current density filaments that can be considered as self-organized quasiparticles, and, on the other hand, there are current density domains [15,17]. This gas discharge system has been simulated with a two-dimensional fluid model, treating electron and ion dynamics by continuity and transport equations. These particle density equations are coupled via Poisson's equation [18,19]. Both periodic patterns of filaments and solitary filaments were found in the system using this fluid model [20].

The gas discharge system investigated experimentally consists of a planar arrangement of two glass plates which enclose a gas layer. The glass plates are electrically

contacted on their outer surfaces. One of these contacts is transparent. Therefore, the light emitted from the gas discharge space can be recorded optically. It is a measure for the current density in the gas. Glass plates and gas gap have a thickness of about 0.5 mm each, whereas the lateral extension of the active region lies in the range of 5–50 mm. The system is supplied by a 200 kHz sinusoidal ac voltage with voltage amplitudes up to 1 kV.

We measure the global luminous intensity with the aid of a photomultiplier device and examine the lateral distribution of the emitted light with video or high-speed cameras, including a framing camera system allowing for the recording of two-dimensional light intensity distributions with a time resolution down to 300 ns. By observing the luminous intensity distribution through the transparent electrode, we average its intensity distribution in a direction perpendicular to the electrodes. We thus neglect the formation of transient glow discharges in the gas gap and treat the device as a quasi-two-dimensional system.

For appropriate system parameters, a single filament can be stabilized on the active area. Such a current density filament has a diameter of about 1 mm and is therefore small compared to the size of the active region. Depending on the parameters, a filament can be stationary or in motion, usually at a speed of some mm/s.

In the present paper we are concerned with a destabilization process of single filaments: in a gas mixture of  $p_{\text{He}} = 350$  hPa and  $p_{\text{air}} = 33$  hPa ( $1 \text{ hPa} = 10^2 \text{ Pa}$ ), single current density filaments are observed in a certain voltage range. If the voltage amplitude is decreased, starting with one circular filament, the latter can undergo a transition towards a dumbbell-shaped filament. Figure 1(a) shows examples of spatially resolved luminous density distributions and their profiles of both a rotationally symmetrical and a dumbbell-shaped filament. Filaments of dumbbell shape may be stationary or perform a rotational motion on a time scale of seconds.

In a first step, we are interested in which way the global brightness of a filament depends on the supply voltage. The upper voltage limit for the existence of single solitary filaments in the above mentioned gas mixture is 680 V. At higher voltages, further filaments are generated. Starting

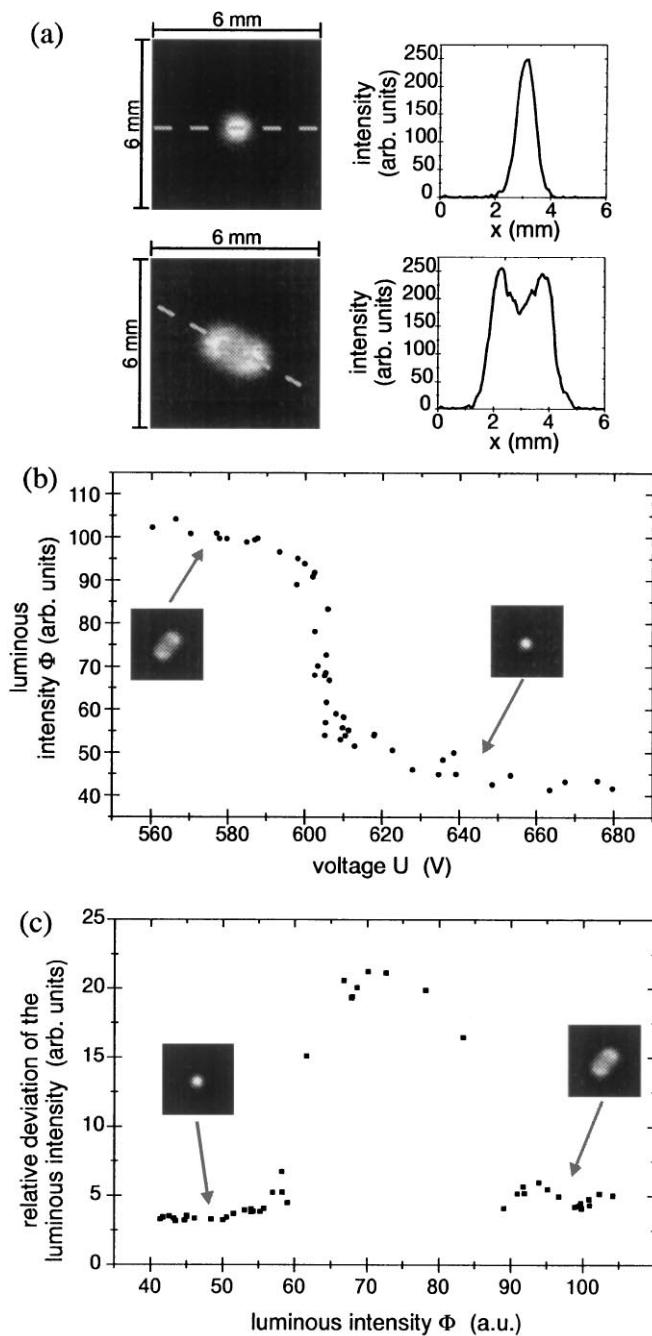


FIG. 1. Global behavior of a filament undergoing a transition from a circular to a dumbbell-shaped state. (a) Two examples of circular and dumbbell-shaped filaments and their profiles. The pictures show luminous intensity distributions lateral to the current flow. (b) Dependence of the global luminous intensity on the voltage amplitude. The pictures show the spatial distribution of the filaments in the low- and high-intensity states, respectively. In the steep transition range the filament occupies a qualitatively different state. (c) Relative fluctuation of the luminous intensity of the filament. Again the pictures indicate the form of the filament in the corresponding branch of the luminous intensity. The range of high deviation corresponds to the steep transition range in plot (b). Parameters: gas-gap thickness 0.5 mm, dielectric thickness 0.55 mm each, system's diameter 10 mm,  $f = 180$  kHz,  $p = 350$  hPa helium + 33 hPa air,  $U = 605$  V, exposure time  $50 \mu\text{s}$ .

from this point, the voltage amplitude was decreased and time series of the global luminous intensity of the filament were recorded at constant voltage and then averaged over a time period of 50 ms. This global, long time scale intensity of the filament slightly increases towards lower voltages [Fig. 1(b)]. This increase is significant for the gas mixture investigated. At a voltage amplitude of 607 V, a sharp transition takes place: the global intensity grows by a factor of approximately 1.4 within a voltage interval of 5 V leading to the state of a dumbbell-shaped filament. A further decrease of the voltage once again leads to a slight growth of the filament's brightness. At 560 V, the filament vanishes abruptly. Although the phenomenon itself is reproducible, the exact voltage value at which the transition occurs depends very sensitively on the gas mixture.

If the filament is not extinguished but the voltage raised opportunely, the luminous intensity follows the same dependence on the voltage in the reverse direction without measurable hysteresis.

To get a first impression of the dynamic range of a filament's luminous intensity, one may look at the standard deviation of its temporal evolution. In Fig. 1(c) the standard deviation with respect to the mean intensity, again calculated for a period of 50 ms, is plotted versus the global intensity. It turns out that the relative deviation of the luminous intensity of circular as well as of dumbbell-shaped filaments is more or less constant in the entire voltage range of their existence. In the intermediate transition range, the deviation is considerably higher. The sharp transitions between the intermediate luminous intensity state and the low- and high-intensity states, respectively, indicate that the intermediate state belongs to a completely separate mode and does not represent a smooth transition between circular and dumbbell-shaped filaments.

We now take a closer look at the spatiotemporal evolution of the different filament states in order to clarify the bifurcation scenario described above. Figure 2(a) shows a typical time series of the global luminous intensity of a filament in the intermediate voltage range. In this time series, one finds two characteristic levels of the luminous intensity corresponding to circular and deformed filaments, respectively. The filament stays in one of the states for several milliseconds and then undergoes a transition towards the other filament state within 50–100  $\mu\text{s}$ . The two levels of brightness of the given time series differ by a factor of about 1.4. This matches the ratio of the end and starting points of the low- and high-intensity branches of Fig. 1(b).

In addition to the global measurement carried out, the discharge was observed with the framing camera system. Figure 2(b) shows the evolution of the filament's spatial distribution. The time of measurement of each picture represented in Fig. 2(b) is matched in Fig. 2(a). The state of low luminous intensity corresponds to filaments of

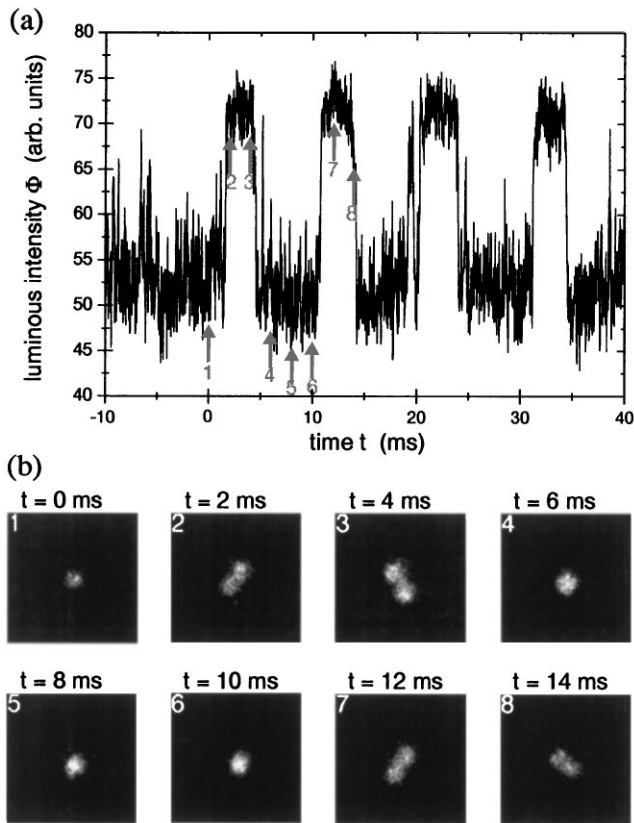


FIG. 2. Spatiotemporal evolution of a breathing filament. (a) Typical time series of the global luminous intensity of a filament in the transition range from circular to dumbbell-shaped filaments. (b) Spatial distribution of the filament at different times of measurement. The corresponding numbers are indicated in (a). Parameters: gas-gap thickness 0.5 mm, dielectric thickness 0.55 mm each, system's diameter 20 mm,  $f = 184$  kHz,  $p = 350$  hPa helium + 32 hPa air, exposure time 50  $\mu$ s.

rotational symmetry, while the filaments in the state of high intensity are of a dumbbell shape. We therefore have to deal with a breathing motion between the two characteristic filament states. We talk of a breathing motion because it is only the filament's extension which oscillates, while its amplitude stays approximately constant. Figure 2(b) shows an example in which the filament breathes and rotates at the same time.

A closer look at the transition shows that a dumbbell-shaped filament having two maxima turns into an elliptically deformed filament with only one maximum in the luminous intensity. This deformed filament then decreases in eccentricity and reaches the state of a circular filament. By taking frames of dumbbell-shaped filaments with an exposure time of one half-cycle of the driver period we could exclude a rocking motion of a single filament leading to a two-armed filament on a longer time scale.

The filament's global brightness was investigated with regard to characteristic oscillation frequencies. The Fourier transforms of the time series indicate that the

fluctuations of circular filaments are mainly stochastic. There is, however, one characteristic frequency peak of relatively low amplitude in each Fourier transform. In Figs. 3(a) and 3(b) frequency and corresponding power are represented in dependence of the supply voltage. The oscillation frequency decreases monotonously with falling voltage before the bifurcation point to the intermediate state occurs.

Beyond the bifurcation point towards the intermediate state the periodic oscillations continue at growing amplitude. The frequency branch of circular filaments continues to fall towards lower voltage amplitudes reaching a value of about 300 Hz. Parallel to this, a second peak at a higher frequency level occurs. This peak consists of a whole band of frequencies with an approximate half-width of 500 Hz. The local maximum of this frequency band is also represented in Fig. 3(a). The level of the power integrated over the whole frequency band is higher than the power of the low frequency branch. In the range of stable

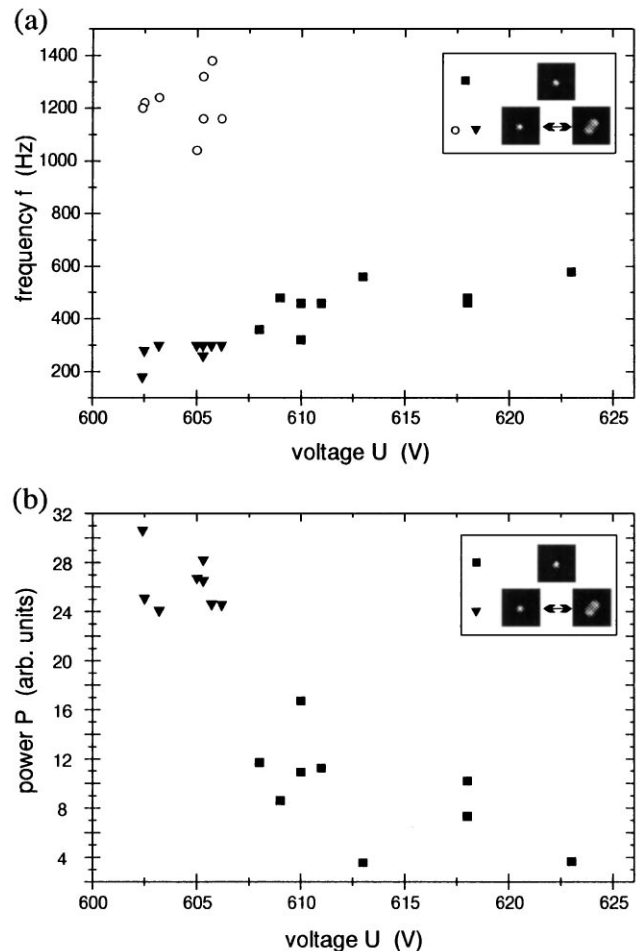


FIG. 3. Characteristic oscillation frequencies of a filament. (a) Dependence of the frequency  $f$  on the voltage amplitude  $U$ . Squares correspond to circular filaments, circles and triangles to filaments in the transition state. (b) Power of the frequency peaks shown in plot (a). Parameters: dimensions as in Fig. 1,  $f = 180$  kHz,  $p = 350$  hPa helium + 33 hPa air.

dumbbell-shaped filaments, no characteristic frequencies could be detected.

In this paper, we have presented results of experimental studies of a dielectric barrier discharge system showing a novel kind of breathing filaments. To describe current density patterns in the above experimental system, it is best to use the semimicroscopic fluid model which has already been applied successfully to take account of standing nonbreathing filaments [20]. This model is based on the diffusion and drift of the charge carriers and the underlying S-shaped current-voltage characteristic. We believe that, in principle, it is also possible to reproduce breathing filaments within the scope of this model. However, the corresponding calculations are highly time-consuming for two reasons: the simulations have to be carried out on a three-dimensional space and, in addition, a periodically driven system has to be dealt with. This means that at least  $10^3$  highly discretized cycles are to be calculated to observe a breathing motion of a period in the order of ms. Both arguments together lead us to the conclusion that, at present, the phenomenon observed cannot be simulated in reasonable time.

A second description of lateral barrier gas discharge systems, originally for dc-driven systems, has been developed on strongly phenomenological grounds. In this activator-inhibitor model, the activator corresponds to the current density in the discharge gap and the inhibitor corresponds to the drop in voltage at the barrier [21].

The phenomenological model was able to reproduce many patterns and bifurcation scenarios observed experimentally in lateral dc discharge systems [8,22,23]. One of the predictions of the two-component model is the bifurcation of a single stationary filament to a breathing one when the inhibitor relaxation time is increased [3,9]. This is just what is observed in the present ac experiments.

Surprisingly enough, the scenario of patterns observed in ac systems is very similar to that of dc systems, in particular, as far as the above-mentioned patterns [6,15,17] are concerned. Therefore, we believe that the fundamental structure of a phenomenological model for ac systems is very similar to that of the phenomenological dc models. This is the case despite the fact that the mechanism which is considered responsible for the formation of current density filaments is somewhat different on a semimicroscopic level. This, in turn, is related to the wall charges at the surface of the dielectrics, which play the role of both activator and inhibitor in ac systems, depending on the moment of time during the half-cycle of the driver [20]. Although there are slight differences between the systems, the similarities in the pattern-forming behavior lead us to the conclusion that breathing filaments might also be ex-

pected in ac systems on the basis of a phenomenological activator-inhibitor model.

We gratefully acknowledge the support of this work by the Deutsche Forschungsgemeinschaft.

- 
- [1] H. Meinhardt, Rep. Prog. Phys. **55**, 797 (1992).
  - [2] J.D. Murray, *Mathematical Biology* (Springer, Berlin, 1980).
  - [3] T. Ohta, M. Mimura, and R. Kobayashi, Physica (Amsterdam) **34D**, 115 (1989).
  - [4] M. Bode and H.-G. Purwins, Physica (Amsterdam) **86D**, 53 (1995).
  - [5] F.-J. Niedernostheide, M. Ardes, M. Or-Guil, and H.-G. Purwins, Phys. Rev. B **49**, 7370 (1994).
  - [6] M. Or-Guil, E. Ammelt, F.-J. Niedernostheide, and H.-G. Purwins, Pitman Research Notes in Mathematics Series **335**, 223 (1995).
  - [7] K. Krischer and A. Mikhailov, Phys. Rev. Lett. **73**, 3165 (1994).
  - [8] C.P. Schenk, M. Or-Guil, M. Bode, and H.-G. Purwins, Phys. Rev. Lett. **78**, 3781 (1997).
  - [9] S. Koga and Y. Kuramoto, Prog. Theor. Phys. **63**, 106 (1980).
  - [10] D. Haim, G. Li, Q. Ouyang, W.D. McCormick, H.L. Swinney, A. Hagberg, and E. Meron, Phys. Rev. Lett. **77**, 190 (1996).
  - [11] M. Gorman, M. El-Hamdi, and K.A. Robbins, Combust. Sci. Technol. **98**, 47 (1994).
  - [12] K. Buss, Arch. Elektrotech. **20**, 261 (1932).
  - [13] U. Kogelschatz, B. Eliasson, and W. Egli, J. Phys. IV (France) **7**, C4-47 (1997).
  - [14] Ch. Radehaus, T. Dirksmeyer, H. Willebrand, and H.-G. Purwins, Phys. Lett. A **125**, 92 (1987).
  - [15] E. Ammelt, D. Schweng, and H.-G. Purwins, Phys. Lett. A **179**, 348 (1993).
  - [16] W. Breazeal, K.M. Flynn, and E.G. Gwinn, Phys. Rev. E **52**, 1503 (1995).
  - [17] I. Müller, E. Ammelt, and H.-G. Purwins, in *Proceedings of the XXIII International Conference on Phenomena in Ionized Gases, Toulouse, France, 1997* (Université Paul Sabatier, Toulouse, France, 1997).
  - [18] J. Meunier, P. Belenguer, and J.P. Boeuf, J. Appl. Phys. **78**, 731 (1995).
  - [19] C. Punset, J.P. Boeuf, and L.C. Pitchford, J. Appl. Phys. **83**, 1884 (1998).
  - [20] I. Müller, C. Punset, E. Ammelt, H.-G. Purwins, and J.P. Boeuf, IEEE Trans. Plasma Sci. (to be published).
  - [21] H.-G. Purwins, G. Klempt, and J. Berkemeier, Festkörperprobleme **27**, 27 Vieweg (1987).
  - [22] H.-G. Purwins, C. Radehaus, and J. Berkemeier, Z. Naturforsch. A **43**, 17 (1988).
  - [23] C. Schenk, P. Schütz, M. Bode, and H.-G. Purwins, Phys. Rev. E **57**, 6480 (1998).